Vector tracking aiding for carrier phase estimation in the presence of ionospheric scintillation

Lina Deambrogio, Christophe Macabiau

Vector Tracking Aiding for Carrier Phase Estimation in the presence of Ionospheric Scintillation

Lina Deambrogio, Christophe Macabiau,
ENAC/Université de Toulouse, Toulouse, France

BIOGRAPHY

Lina DEAMBROGIO received the Master degree in Telecommunication Engineering in 2007 and the PhD in 2012 both from the University of Bologna, Italy. From March 2012 she is a researcher in the signal processing lab of ENAC in Toulouse, France. Her research area is the study of signal processing techniques for GNSS receivers in degraded scenarios.

Christophe MACABIAU graduated as an electronics engineer in 1992 from the ENAC in Toulouse, France. Since 1994, he has been working on the application of satellite navigation techniques to civil aviation. He received his PhD in 1997 and has been in charge of the signal processing lab of ENAC from 2000 to 2012. He is currently the head of the TELECOM lab of ENAC.

ABSTRACT

In GNSS receivers, the ability of guaranteeing continuous position, velocity and time (PVT) solutions is linked with their capacity of maintaining lock with the satellite signals. However, this is not always possible and in degraded environments the received signals can be strongly attenuated or affected by errors that cause the tracking loops to lose lock and the navigation processor to be unable to produce a useful positioning solution.

A particularly challenging environment is represented by the presence of ionospheric scintillations that combine signal fading and fast phase variations. These effects can severely test receiver tracking loops and their capacity to follow the received signal changes. Carrier tracking through phase lock loops (PLL) is especially susceptible to losing lock. Amplitude scintillations may in fact generate deep fades in the received signal power that in worst cases can cause the signal to drop below the lock threshold; on the other hand, phase scintillations cause rapid carrier phase changes that might produce cycle slips and even cause loss of lock.

This lack of robustness strongly impacts receiver performance as it reduces carrier phase measurements availability, the capability to demodulate the navigation message data and the ability to perform carrier-smoothing.

This is the motivation behind the study of innovative architectures to improve receiver robustness and aid the phase tracking process. Ionospheric scintillation mitigation can in fact be achieved by improving carrier tracking ability to sustain rapidly changing received signals.

Different tracking schemes could be envisaged; in this paper a Vector Frequency Lock Loop (VFLL) assisted PLL is described. Vector tracking loops are interesting as they allow implementing cross-channel aiding by linking together all received signals through the receiver position and velocity. The aim of this paper is therefore to present the VFLL-assisted PLL receiver architecture describing the system model and feedback generation process and to test its feasibility in scintillation scenarios. To reproduce the scintillation effect, the Cornell Scintillation Model (CSM) has been used and simulations that quantify the performance in terms of phase tracking error variance, cycle slips and loss of lock are conducted.

INTRODUCTION

I. IONOSPHERIC SCINTILLATIONS

The ionosphere is a layer in the upper atmosphere characterized by the presence of free electrons generated by solar radiations. In nominal conditions, signals propagating through the ionosphere get refracted experiencing a delay in the code and an advance in the carrier phase. However, in the presence of high solar activity, disturbances and irregularities may originate within the ionosphere causing rapid fluctuations in the received signals. Indeed, the presence of anomalies in the refraction index can cause the signals to scatter in random directions inducing amplitude and phase scintillations. At the receiver, the combination of the scattered signal paths

produces amplitude scintillations, which consist in both deep signal fades and shallow enhancements, and phase scintillations that are observed as rapid fluctuations in the carrier phase shift [1].

The received GNSS signal affected by scintillation can therefore be modeled as:

$$r(t) = A_0 \delta A c(t-\tau) d(t-\tau) \cos(2\pi f_0 t - \theta - \delta\varphi) + n(t) \quad (1)$$

Where:

- A_0 is the nominal amplitude of the signal
- f_0 is the nominal carrier frequency
- d(t) is the waveform encoding the navigation message
- c(t) is the waveform encoding the PRN code
- τ is the propagation delay
- $\theta=\Phi-2\pi f_0\tau$ is the received carrier phase delay
- Φ is the initial phase
- δA is the scintillation amplitude
- $\delta\varphi$ is the scintillation phase
- $n(t)$ is the additive white noise

Scintillations can be described through probability distributions. The fluctuations in the signal intensity are generally modeled as following a Nakagami-m distribution with mean value 1 and variance $1/m$ [2]:

$$p(I) = \frac{m^m \delta I^m}{\Gamma(\mathrm{m})} e^{-m\delta I} \quad (2)$$

Where $I = A^2 = [A_0 \delta A]^2$ and $\delta I \geq 0$.

The effects of amplitude scintillations are characterized by the S_4 index that is the normalized standard deviation of the fluctuating received signal power:

$$S_4 = \sqrt{\frac{1}{m}} = \frac{\sqrt{Var(I)}}{E[I]} \quad (3)$$

Due to properties of Nakagami distributions the constraint $S_4 \leq \sqrt{2}$ is introduced.

Phase scintillations follow a zero mean Gaussian distribution characterized by the standard deviation σ_ϕ:

$$p(\phi) = \frac{1}{\sqrt{2\pi}\sigma_\phi} e^{\frac{-\phi^2}{2\sigma_\phi^2}} \quad (4)$$

Amplitude and phase scintillations are both highly correlated over short intervals.

Moreover, it should be noted that scintillation affects signals in different bands differently and the scintillation parameters follow the trends:

$$S_4 \propto \frac{1}{f^{1.5}} \quad \text{and} \quad \sigma_\phi \propto \frac{1}{f}$$

Scintillations are influenced by the solar activity but also by the Earth's magnetic field causing scintillations to be more frequent and severe in the region around the equator. In the following only equatorial scintillations will be considered.

Finally, it should be pointed out that due to the irregular nature of the disturbances in the ionosphere, not all satellites in view may be affected by scintillations at the same time.

II. SCINTILLATION MODELS

In literature, different models have been defined for scintillation prediction that can be used to evaluate the performance of a system in different scintillation scenarios. However, the models only provide a global scintillation representation based on values observed at different instants of the solar cycle. Moreover, it is worthwhile noting that these models are usually limited to equatorial scintillation.

A. Simplified Model

A simplified model can be implemented by assuming the scintillation amplitude as following a Gamma distribution that approximates the Nakagami-m distribution. The Gamma distribution can be obtained by setting its parameters to $\alpha = 1/\beta = 1/S_4^2$ [3] [4].

Phase scintillations can be modeled following a Gaussian distribution as defined in section I.

B. WBMOD

The Wide Band Model (WBMOD) is a model developed by NWRA with the support of the US government to estimate the severity level of the effects of scintillations on systems in particular environmental conditions. It consists of two parts: an electron density irregularities model and a propagation model [5]. The electron density model was developed based on a large collection of scintillation observations (Wideband, HiLat and Polar Bear experiences, USAF monitoring network) which is feed to an empirical model of electron density obtained as a function of date, time and position but also of solar activity (number of sunspots) and geomagnetic parameters. The propagation model employed is a phase screen model. WBMOD allows to estimate the severity of the effects of the scintillations at a given altitude and plots the corresponding map. However, it does not provide the

classical S_4 and σ_ϕ parameters, estimating instead the probabilities that a scintillation level is reached.

C. GISM

The Global Ionospheric Scintillation Model (GISM) allows computing the scintillation effects on a signal crossing the ionosphere from a GPS satellite to a fixed terrestrial receiver. The model consists of two parts: the background electron density model and the scintillation model based on the multiple phase screens (MPS) algorithm [5]. The medium is divided into successive layers each represented by a phase screen that mimics the irregularities in the ionosphere. The line of sight is first computed considering the different indices of the crossed layers and the incident and refracted angles, finally the electron density at each layer is given by the NeQuick model [6]. A more detailed description of the GISM is given in [7].

The model inputs are:

- The date of the simulations
- The solar flux
- The geographical coordinates at the observation point

The main outputs of the model are:

- The time series of the amplitude and phase of the signals at the selected frequency.
- The estimated S4 and sigma-phi computed every minute.

D. CSM

The Cornell Scintillation Model (CSM) defines amplitude and phase scintillations for equatorial regions.
It is a statistical model which shapes the scattered signals as a zero-mean Complex Gaussian distribution. Amplitude scintillations are assumed as following a Rice distribution. This assumption has been made because of the simplicity of the Rice model implementation. In fact, although the Nakamami-*m* distribution is the one that fits better the real scintillation data, as described in section I, in [8] it is shown that Nakamami-*m* and Rice distribution are similar and agree according to the chi-square test to the empirical data when $S_4 < 1$. Thus, the Nakamagi-*m* distribution can be closely approximated by the Rice distribution [9]. The model inputs are the S_4 level (with a maximum value equal to 1) and the correlation time τ_0, which represents how quickly the signal amplitude and phase change (ranging from 0.1 s to 2s for the GPS L1 frequency, with lower values describing faster changing channels). In the CSM, phase and amplitude scintillations are not modeled independently in order to be able to represent correctly the canonical fades during which rapid phase changes are coupled with deep signal fades.

The CSM is used in the following to generate the scintillation time series used to test the tracking loop robustness. Different levels of severity of ionospheric scintillation have been considered to test the receiver robustness [10]:

- Weak scintillations characterized by S_4=0.51 and τ_0=0.71
- Moderate scintillations characterized by S_4=0.69 and τ_0=0.18
- Severe scintillations characterized by S_4=0.87 and τ_0=0.18

The following figures show the amplitude and phase time series obtained through the CSM in the three different scenarios defined above. It should be noted that increasing values of S_4 are linked to wider ranges of scintillation amplitudes, while smaller values of τ_0 generate faster changing phases and in extreme conditions, as in Figure 6, generate fast jumps in the phase that can be very challenging for a PLL to follow.

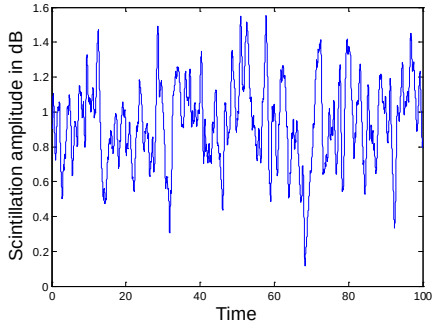

Figure 1 Scintillation amplitude for the weak scintillation scenario with S4=0.51 and τ0=0.71

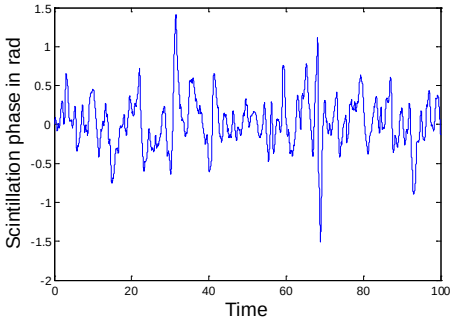

Figure 2 Scintillation phase for the weak scintillation scenario with S4=0.51 and τ0=0.71

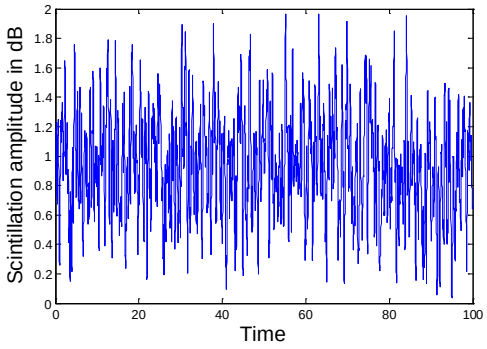

Figure 3 Scintillation amplitude for the moderate scintillation scenario with S4=0.69 and τ0=0.18

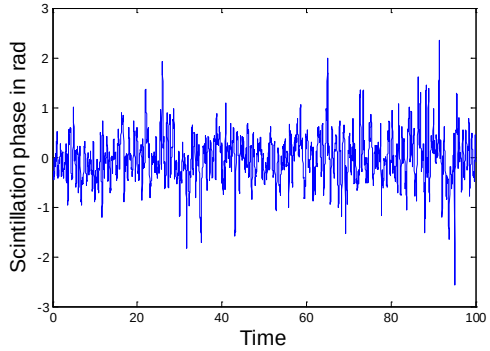

Figure 4 Scintillation phase for the moderate scintillation scenario with S4=0.69 and τ0=0.18

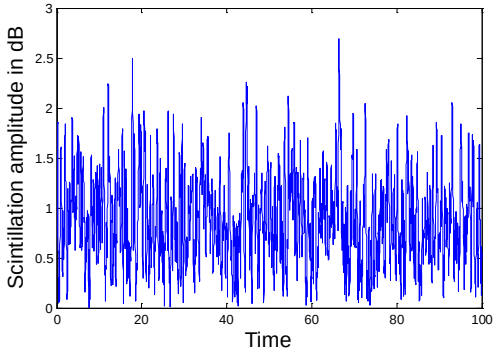

Figure 5 Scintillation amplitude for the severe scintillation scenario with S4=0.87 and τ0=0.18

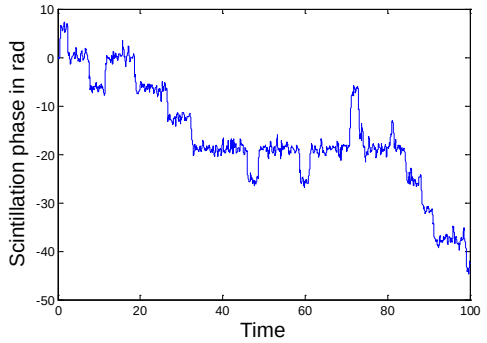

Figure 6 Scintillation phase for the severe scintillation scenario with S4=0.87 and τ0=0.18

III. SCINTILLATION IMPACT ON TRACKING LOOPS

As mentioned before, fluctuations in the signal intensity, and thus signal amplitude, can in severe cases cause the loss of tracking lock. Also the rapid phase variations can result in a loss of lock if they exceed the bandwidth of the PLL.

In [11] the effects of amplitude and phase scintillation on the transmitted signal are considered as independent:

- The effect on the amplitude is modelled as an increase in thermal noise due to a decrease in signal power;
- The effect on the phase is considered as an additive term to the overall variance of the tracking phase error.

The σ_ϕ index, which is computed as the standard deviation of the phase tracking error at the output of the Phase Lock Loop (PLL) circuit, can be modeled as the square root of the sum of three terms:

$$\sigma_\phi^2 = \sigma_{\phi_T}^2 + \sigma_{\phi_P}^2 + \sigma_{\phi_{osc}}^2 \tag{5}$$

- $\sigma_{\phi T}^2$ is the contribution due to thermal noise and can be derived as:

$$\sigma_{\phi_T}^2 = \frac{B_n\left[1 + \frac{1}{2T_i CNo\left(1 - S_4^2(L1)\right)}\right]}{CNo\left(1 - S_4^2(L1)\right)} \tag{6}$$

Where:

  - B_n is the PLL loop bandwidth
  - T_i is the integration time
  - $S_4 < 0.707$ in order for the equation to be defined

- $\sigma_{\phi_P}^2$ is the phase scintillation variance

$$\sigma_{\phi_P}^2 \cong 2\int_0^\infty |1 - H(f)|^2 S_{\hat{\phi}}(f) df \tag{7}$$

Where $S_{\hat{\phi}}$ is the Power Spectral Density (PSD) of the phase scintillation and $|1 - H(f)|^2$ is the closed loop transfer function of the PLL that depends on k, the loop order, and f_n, the loop natural frequency.

$$|1 - H(f)|^2 = \frac{f^{2k}}{f^{2k} + f_n^{2k}} \quad (8)$$

Typical values are k = 3 and f_n= 1.91 Hz [12].

- And $\sigma^2_{\phi_{osc}}$ is the contribution due to the receiver oscillator noise.

These indices can be computed over time, and their estimates are generally based on averages obtained over a few tens of seconds. In order to reflect the effect of the scintillation only, it is usually required to remove low frequency variations due to the change of the distance between the satellite and the receiver and local oscillator.

Figure 7 reports the estimated C/N0 for two satellite signals with nominal power equal to 35dBHz. The effect of scintillation (generated with the CSM considering S_4=0.69 and τ_0=0.18) causes the affected signal to have a considerable drop in received signal power that may become too low for the tracking circuit and generate loss of lock events.

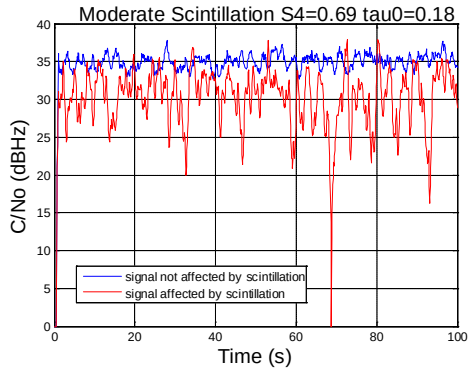

Figure 7 Impact of scintillation on received signal power

Alternatively, loss of lock can be caused also by rapid transitions in the phase of the received signal. Figure 8 reports on the top plot the behavior of the carrier phase error (computed as the difference between the received carrier phase affected by scintillation and the estimated carrier phase) while the bottom plot shows the corresponding injected scintillation. As shown, the rapid changes in the received signal phase cause the generation of cycle slip events and may in extreme cases lead to the loss of lock.

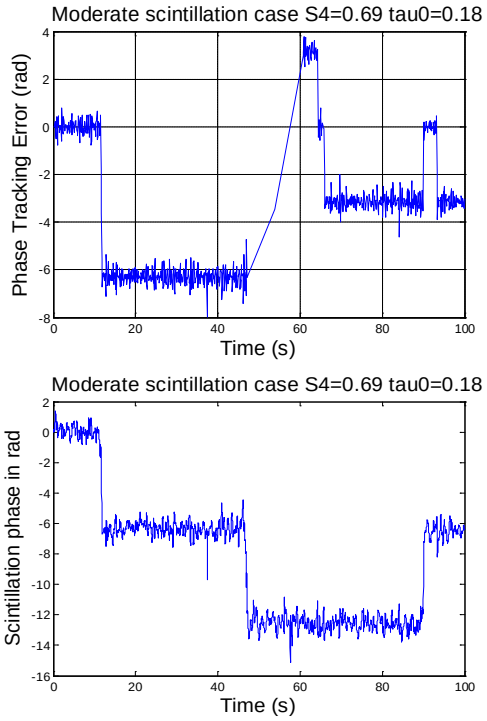

Figure 8 Impact of scintillation on signal phase

MITIGATION TECHNIQUES

As shown, in GNSS receivers, the carrier tracking block through PLLs is especially susceptible to losing lock in the presence of scintillations. Indeed amplitude scintillations may generate deep fades in the received signal power that in worst cases can cause the signal to drop below the lock threshold; on the other hand, phase scintillations cause rapid carrier phase changes that might produce cycle slips and even cause loss of lock if the variations are too rapid for the loop to follow.

In order to improve carrier phase tracking robustness, that is the ability of the loops to remain locked without needing a re-acquisition procedure, different techniques can be implemented (both scalar and vector).

As a first step to improve performance, a PLL with tuned parameters can be implemented. The PLL bandwidth can in fact be chosen as the trade-off between the need to limit the increase in noise floor due to amplitude scintillations and the need to follow the rapid changes caused by phase scintillations.

In order to improve further carrier tracking robustness, Frequency Lock Loop (FLL) assisted PLL [13] can be used. In this architecture the loop filter uses two discriminator outputs: one that outputs the frequency error and the other that outputs the phase error. The frequency

aid allows keeping track of the signal even when phase lock is lost. Additionally also Doppler aiding information provided by external sensors [14] could be used.

These types of traditional tracking loops have all constant loop bandwidths. The fine tuning of the loops parameters may increase the robustness of carrier phase tracking but a trade-off has still to be reached between accuracy and robustness. The use of Kalman filters in place of loop discriminator and filters allows overcoming this limitation by dynamically adjusting the weights of the different measurements. Moreover, employing an a priori model of the receiver dynamics permits also to gap low signal-to-noise ratio (SNR) intervals [15].

Finally vector tracking architectures can also be implemented. Differently from traditional receivers, vector tracking is based on processing all received signals collectively and using the navigation filter outputs as feedback to drive the loop code and carrier generators [16].

Vector tracking loops are especially interesting as they allow to implement cross-channel aiding by linking together all received signals through the receiver position and velocity. Using the navigation processor outputs it is in fact possible to exploit the stronger signals to aid the weaker ones thus helping them to remain locked even when affected by errors or strongly attenuated. The navigation processor becomes thus the block in charge of closing the tracking loops and providing the tracking control information to drive the numerically controlled oscillators (NCO).

Cross-channel aiding is particularly appealing in the presence of ionospheric scintillations since just some of the satellites in view might be affected by scintillation and be degraded.

The feedback provided by the navigation filter could, in principle, be used both for predicting code and carrier phases. Nevertheless, it should be noted that carrier phase tracking poses additional challenges. The estimated position or estimated change of position, in fact, is not sufficiently accurate to unambiguously predict the phase of the carrier signals, because of the impact of propagation errors (tropospheric and ionospheric delays) and satellite clock bias. The demand on position or position update accuracy becomes thus quite stringent and hard to provide in order to guarantee that the errors affecting the position estimate are in the cm-level order.
Due to the difficulties in implementing a pure VPLL, the literature lacks a common baseline and different schemes have been proposed [17] [18] [19] [20].

In this work we consider the feasibility of a carrier tracking scheme based on a Vector Frequency Lock Loop (VFLL) to achieve robust frequency tracking. In order to execute carrier phase tracking, aiding from the VFLL outputs is provided in a VFLL-assisted PLL architecture thus combining the robustness of vector frequency tracking that exploits cross-channel aiding with the accuracy of PLL carrier phase tracking [21]. This combination feeds the carrier NCO with outputs from both the VFLL and PLL discriminators and filters. This way the VFLL is in charge of tracking the line-of-sight (LOS) dynamics and the PLL has just to track the residual carrier mismatch.

Vector configurations can rely on different types of realizations depending on the navigation filter implemented. In general both Least Squares estimators and Kalman filters can be employed.

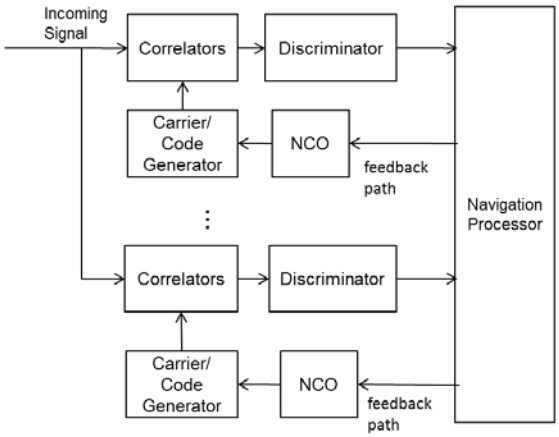

Figure 9 Generic vector tracking architecture

ALGORITHM DESCRIPTION

In the present work, the scheme implemented follows the definition in [21]. In this case the VFLL does not directly control the carrier NCOs but is used to provide refined versions of FLL discriminator outputs. The refined values are then filtered and together with the filtered PLL discriminators are used to steer the NCO and achieve phase lock for all channels, as shown in Figure 2.
In the figure Δf_i and $\Delta \hat{f}_i$ indicate the FLL discriminator output and the refined discriminator output respectively, while $\Delta \phi_i$ is the PLL discriminator output.

The FLL discriminator outputs are computed as:

$$\Delta f_i = \tan^{-1}\left(\frac{Q_{P_1}}{I_{P_1}}\right) - \tan^{-1}\left(\frac{Q_{P_2}}{I_{P_2}}\right) \quad (9)$$

Where:

- I_{P_1}, I_{P_2} are the in-phase components of the prompt correlator taken at two consecutive time intervals $t_1$and t_2
- Q_{P_1}, Q_{P_2} are the quadrature components of the prompt correlator taken at two consecutive time intervals $t_1$and t_2

The PLL discriminator is computed as:

$$\Delta\phi_i = \tan^{-1}\left(\frac{Q_P}{I_P}\right) \tag{10}$$

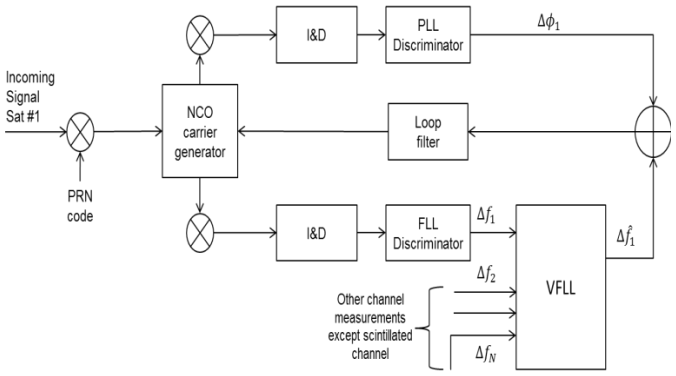

Figure 10 Implemented VFLL-assisted PLL architecture

It must be noted that only the signals not affected by scintillation (signals that have not lost PLL lock) are considered as inputs in the VFLL solution. This is because any error affecting one channel can potentially adversely degrade the navigation solution and thus impact all other channels. It is therefore fundamental to monitor the received signal quality in order to disconnect the corrupted signals from the common loop.

The metric used in the present work to recognize signals that lose lock is the Phase Lock Indicator (PLI) defined in [16]:

$$\cos(2\phi) = \frac{|\sum_M I_P|^2 - |\sum_M Q_P|^2}{|\sum_M I_P|^2 + |\sum_M Q_P|^2} = \begin{cases} 1 \; locked \\ < 0.4 \; loss \; of \; lock \end{cases} \tag{11}$$

The VFLL block has been implemented through a Least Squares (LS) estimator as detailed in the following Figure 3.

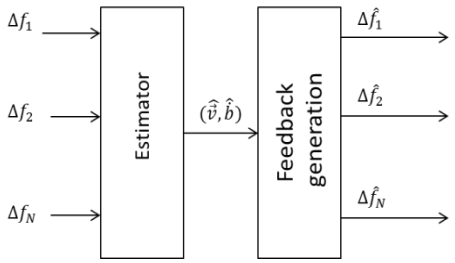

Figure 11 VFLL implementation

All reliable discriminator output measurements are processed in the LS to obtain an estimation of the receiver velocity and clock drift bias. The estimated velocity and clock bias are then used to compute refined discriminator outputs that will then be filtered and together with the PLL used to pilot the NCO. For each channel the refined discriminators are computed as:

$$\Delta \hat{f}_i = \frac{(\hat{\vec{v}} - \hat{\vec{v}}_{sat,i})\vec{a}_i - \hat{b}}{\lambda} \tag{12}$$

Where:

- $\hat{\vec{v}}$ is the receiver velocity computed by processing the measurement provided by the uncorrupted received measurements
- $\hat{\vec{v}}_{sat,i}$is the i-th satellite velocity
- $\vec{a}_i$ is the unit vector pointing from the user to the i-th satellite
- $\hat{b}$ is the estimated receiver clock drift
- λ is the signal wavelenght

For each channel i the computed discriminator $\Delta \hat{f}_i$ replaces the FLL discriminator and is filtered in a standard fashion through the loop-filter before steering the carrier NCO. Ultimately the adopted scheme provides a vector FLL that employs traditional loop filters to reduce noise and to accurately replicate the satellite signal.

A third order PLL is assisted by a second order FLL making the carrier tracking loop insensitive to acceleration stress but sensitive to jerk stress.

NUMERICAL RESULTS

The proposed algorithm has been tested considering different types of scintillation time series generated with the CSM:

- Weak scintillations characterized by S_4=0.51 and τ_0=0.71

- Moderate scintillations characterized by S_4=0.69 and τ_0=0.18
- Severe scintillations characterized by S_4=0.87 and τ_0=0.18

A ground static receiver has been simulated, with a visibility of six satellites one of which is affected by scintillation.

Two different levels of C/N0 have been considered for all satellites: 35 dBHz and 40dBHz.

Simulations have been carried out for 100s and the receiver oscillator considered is a TCXO.

A. WEAK SCINTILLATION CASE

Scintillation scenario	Type of tracking	C/N0 (dBHz)	Phase error std	Cycle slips	Re-acquisitions
Weak S_4=0.51 τ_0=0.71	scalar	35	0.07 rad/4 deg	0	0
	scalar	40	0.05 rad/3 deg	0	0
	vector	35	0.07 rad/4 deg	0	0
	vector	40	0.05 rad/3 deg	0	0

Table 1 Performance of the carrier phase tracking loop in the presence of weak scintillations

The performance reported in Table 1, shows clearly that the weak scintillation case does not pose problems to PLL circuits. Since no loss of lock of the PLL takes place, the VFLL is never triggered and the standard deviation of the phase error is the same in the two cases.

B. MODERATE SCINTILLATION CASE

Scintillation scenario	Type of tracking	C/N0 (dBHz)	Phase error std	Cycle slips	Re-acquisitions
Moderate S_4=0.69 τ_0=0.18	scalar	35	0.32 rad/ 18 deg	11	2
	scalar	40	0.29 rad/ 16 deg	5	0
	vector	35	0.31 rad/ 17 deg	12	0
	vector	40	0.29 rad/ 16 deg	4	0

Table 2 Performance of the carrier phase tracking loop in the presence of moderate scintillations

In the presence of moderate scintillations, Table 2, at low C/N0 values there are actually loss of lock events that trigger the VFLL. Vector tracking assistance allows in these cases to effectively maintain lock by employing cross-channel aiding. Performance in terms of carrier phase accuracy are not improved, however it should be noted that in FLL-assisted PLL configurations the burden of following the Line Of Sight (LOS) is delegated to the FLL but no phase lock is achieved. In these cases, the PLL has to estimate the residual mismatch that is in general larger than when tracking with PLL only.

C. SEVERE SCINTILLATION CASE

Scintillation scenario	Type of tracking	C/N0 (dBHz)	Phase error std	Cycle slips	Re-acquisitions
Severe S_4=0.87 τ_0=0.18	scalar	35	0.47 rad/ 27 deg	200	6
	scalar	40	0.45 rad/ 26 deg	96	6
	vector	35	0.47 rad/ 27 deg	102	5
	vector	40	0.45 rad/ 26 deg	55	2

Table 3 Performance of the carrier phase tracking loop in the presence of severe scintillations

Analogously to the previous case, in the presence of severe scintillations, the robustness of the carrier tracking block is generally improved.

D. FREQUENCY ESTIMATION PERFORMANCE

C/N0 (dBHz)	Scintillation	Frequency error std (Hz) (scalar loops)	Frequency error std (Hz) (vector loops)
35	No	0.33	0.33
	Weak	0.53	0.41
	Moderate	1.12	1.10
	Severe	1.93	1.90
40	No	0.20	0.19
	Weak	0.26	0.24
	Moderate	1.02	0.98
	Severe	1.90	1.84

Table 4 Performance of the carrier frequency tracking loop in the presence of scintillations

By employing a vector tracking configuration, it is possible to improve frequency estimation accuracy. It must be noted that the navigation processor used in this work is a simple LS with no weights or additional information inserted. Performance should improve further by applying assistance information on the receiver.

CONCLUSIONS AND FUTURE DEVELOPMENTS

Ionospheric scintillation can be very challenging for carrier tracking loops as the deep power fades caused by amplitude scintillations and the rapid changes due to phase scintillations can cause the receiver to lose lock of the received signal and require long re-acquisition procedures. In order to improve the robustness of the carrier tracking block, in this paper a vector tracking configuration has been implemented. The VFLL-assisted PLL scheme here described allows in fact to reduce the number of re-acquisitions by exploiting the correlation between all received signals. By linking together all received signals is in fact possible to use the stronger unaffected signals to aid the weaker ones.

Scintillation events offer an interesting scenario as not all satellites in view are affected simultaneously.
Simulation show that for $S_4 \leq 0.5$ PLL tracking can be carried out with no loss of lock events and VFLL-assisted PLL tracking is not triggered. However, for moderate and severe scintillations, VFLL assistance has proven helpful to reduce the number of re-acquisitions events.

Future developments should consider dynamic receivers. In this case, by implementing a Kalman filter as the navigation processor in place of the LS, it will be possible to insert also additional a priori information on the receiver dynamics and tune the filter to the specific scenario yielding better performance.

Moreover, different types of scintillation events (high latitudes and equatorial) should be considered and the behavior of the carrier tracking block tested.

REFERENCES

[1] “Effect of Ionospheric Scintillations on GNSS – A White Paper”, SBAS Ionospheric Working Group (Stanford University), November 2010.

[2] E. D. Kaplan, C. Hegarty, “Understanding GPS: Principles and Applications,” Artech House Mobile Communications Series, 2006.

[3] C. Hegarty, M. B. El-Arini, T. Kim, S. Ericson, « Scintillation modelling for GPS – Wide Area Augmentation System receivers », Radio Science, Vol. 36, N. 5, Sept-Oct. 2001.

[4] F. Ghafoori and S. Skone, « High Latitude Scintillation Analysis for Marine and Aviation Applications », ION GNSS 2012, Session A5.

[5] CIGALA Project State of the art review D2.1-WP200 V1. FINAL VERSION. 7th Framework Program Grant Agreement No:247920

[6] S.M Radicella, B. Nava, "NeQuick model: Origin and evolution," Antennas Propagation and EM Theory (ISAPE), 2010 9th International Symposium on , vol., no., pp.422-425, Nov. 29 2010-Dec. 2 2010 doi: 10.1109/ISAPE.2010.5696491

[7] Y. BENIGUEL, “GISM User manual”, 2010.

[8] T. E. Humphreys, M. L. Psiaki, J. C. Hinks, P. M. Kintner Jr., “Simulating Ionosphere-Induced Scintillation for Testing GPS Receiver Phase Tracking Loops”, IEEE Transactions on Aerospace and Electronic Systems.

[9] A. O. Moraes, and W. J. Pererella, , “Performance evaluation of GPS receiver under equatorial scintillation”, Journal of Aerospace Technology and Management, V. 1, n. 2, Jul.- Dec. 2009.

[10] T. E. Humphreys, M. Psiaki, B. Ledvina, A. Cerruti, P. M. Kitner, “A data-driven simulation testbed for evaluating GPS carrier tracking loops in severe ionospehric scintillation”, IEEE Trans. on Aerospace and Electronic Systems.

[11] R. S. Conker, M. B. El-Arini, C. Hegarty, C.J. and Hsiao, T., “Modelling the Effects of Ionospheric Scintillation on GPS/Satellite-Based Augmentation System Availability”. Radio Sci., 37, 1, 1001, doi: 10.1029/2000RS002604, 2003.

[12] Y. Beniguel, B. Forte, S. M. Radicella, H.J. Strangeways, V. E. Gherm, N. N. Zernov “Scintillations effects on satellite to Earth links for telecommunication and navigation purposes”, Annals of Geophysics, Supplement to Vol. 47, N. 2/3, 2004

[13] P. Ward, “Performance Comparisons Between FLL, PLL and Novel FLL-Assisted PLL Carrier Tracking Loop Under RF Interference Conditions”, Proc. of ION/ITM, Nashville, September 1998.

[14] T. Chiou, J. Seo, T. Walter, and P. Enge, “Performance of a Doppler-Aided GPS Navigation System for Aviation Applications under Ionospheric Scintillation”, in Proc. of ION/ITM, Savannah, GA, 16–19 September, 2008
.
[15] M. L. Psiaki, T. E. Humphreys, A. P. Cerruti, S. P. Powell, and P. M. Kintner, Jr., “Tracking L1 C/A and

L2C Signals through Ionospheric Scintillations", ION GNSS 2007, FT. Worth.

[16] B. W. Parkinson and J. J. Spilker Jr, "Global Positioning Systems: Theory and Applications. Volume I", volume 163, Progress in Astronautics and Aeronautics, 1996.

[17] M.G. Petovello, C. O 'Driscoll, and G. Lachapelle, "Carrier Phase Tracking of Weak Signals Using Different Receiver Architectures," Proceedings of Institute of Navigation National Technical Meeting (ION NTM 2008), 2008.

[18] M. Zhodzishsky, S. Yudanovand, V. Veitsel, and J. Ashjaee, "Co-Op Tracking for Carrier Phase," Proceedings of Institute of Navigation - GPS 98.

[19] P. Henkel, G. X. Gao, T. Walter, and C. Gunther, "Robust Multi-Carrier, Multi-Satellite Vector Phase Locked Loop with Wideband Ionospheric Correction and Integrated Weighted RAIM," Proc. of ENC- GNSS 2009.

[20] S. Peng, Y. J. Morton, R. Dui, "A multiple-frequency GPS software receiver design based on a vector tracking loop", IEEE/ION PLANS 2012, Myrtle Beach, April 23-26, 2012.

[21] S. Kiesel, C. Asher, D. Gramm, and G. F. Trommer, "GNSS Receiver with Vector Based FLL-assisted PLL Carrier Tracking Loop", in Proc. of ION GNSS, 2008.